

DETERMINATION OF THE AERODYNAMIC LIFT FOR A RADIAL ROTOR PASSAGE MODEL USING THE PRESSURE DISTRIBUTION METHOD

SUMMARY

The article presents an attempt to solve the problem of aerodynamic lift in a radial grid of blades experimentally. The blade passage model was tested in a negative pressure wind tunnel and a positive gauge pressure wind tunnel. The lift coefficient in the function of the angle of attack on the inlet blade edge was determined. This study contributes new data to the research on the aerodynamic lift and drag force of blades and radial grids.

Keywords: aerodynamic lift, lift coefficient, blade passage

WYZNACZENIE SIŁY NOŚNEJ DO MODELU KANAŁU WIRNIKA PROMIENIOWEGO METODĄ ROZKŁADU CIŚNIĘŃ

Zagadnienie przedstawione w artykule jest próbą eksperymentalnego rozwiązania problemu siły nośnej w promieniowej palisadzie łopatkowej. Model kanału międzyłopatkowego został przebadany w tunelu aerodynamicznym podciśnieniowym i nadciśnieniowym. Wyznaczono współczynnik siły nośnej w funkcji kąta natarcia strugi na krawędź wlotową łopatki. Jest to część rozważań nad siłą nośną i siłą oporu łopatek i palisad promieniowych.

Słowa kluczowe: siła nośna, współczynnik siły nośnej, kanał łopatkowy

1. INTRODUCTION

Currently, a number of tests are conducted in wind tunnels in the field of fluid mechanics. Their objective is to measure aerodynamic lifts acting on tested objects when they are swilled by fluid. Such tests can also reveal the behaviour of fluid swilling a particular object. In practice, this type of tests can be used in the search for the optimal position of a ski jumper. The ski jumper's speed on reaching the threshold is expected to be the greatest possible, therefore the drag force determined during tests should be the smallest possible component of aerodynamic lifts. This may be possible if an adequate ski position is taken. To be able to jump as far as possible under given weather conditions, a ski jumper should take the position enabling him to have the maximal aerodynamic lift on taking off from the threshold. In addition to measurements aimed to optimize the ski jumper's position, tests of various types of plane wing aerofoils and amphibious vehicle models are carried out. In such tests, the tested object is usually immobilized and fluid is put in motion, though in reality it is the other way round. It is assumed that it does not matter if the tested object is in motion and fluid stationary or vice versa, i.e. fluid in motion and the element fixed.

However, it is not clear if different pressure conditions – negative pressure conditions and positive gauge pressure ones – are of any significance. In other words, it is not known for certain whether or not the value of aerodynamic lift changes along with the type of airflow. The latter can be blowing – when the air moving appliance is placed before the tested object – or suction – when it is placed behind the tested object. In this article, we are trying to determine this issue on the basis of an experiment.

2. METHODS

The measurements of the aerodynamic lift R_Y and lift coefficient C_Y have been carried out for both negative pressure conditions and positive gauge pressure ones in wind tunnels. As the lift coefficient characterises a tested aerodynamic object regardless of the velocity of undisturbed airflow, depending only on the model shape and the angle at which the model is placed in the airflow, it has been used to compare the results of both measurements.

The aerodynamic lift and lift coefficient were determined for a blade passage model of radial fan WWOax 22.5 with nine blades. First, the model was placed in the negative pressure wind tunnel, where the airflow velocity was 18.1 m/s, and the pressure distribution was measured. Then, the model was moved to the positive pressure gauge wind tunnel, where the airflow velocity was 14 m/s, and the pressure distribution was measured again. Different values of airflow velocity are the result of varying technical potential of the two wind tunnels.

Figure 1 shows the wind tunnel of rectangular cross-section $a = 295$ mm, $d = 215$ mm. There was a straightener at the inlet 2. The pressure measured in the blade passage was pulled out to a micromanometer using hoses 1. The airflow was generated by an axial-flow fan 3. The space where the tested object is to be placed is determined by axes $OXYZ$. There is negative pressure in the measuring space. The object was oriented relative to the OX and OY axes with the use of the γ angle setting.

The second positive gauge pressure wind tunnel is shown in Figure 2. In this tunnel, it was possible to achieve air velocity different to that in the previous tunnel. This is substantiated by the tunnel diagram shown in Figure 3. The

* AGH University of Science and Technology in Cracow

axial-flow fan 1 is driven by motor 2. The motor rotational speed was regulated with the use of an inverter 3. The air-flow direction was changed by adequately set stators 4 placed in rectangular turns of the tunnel.

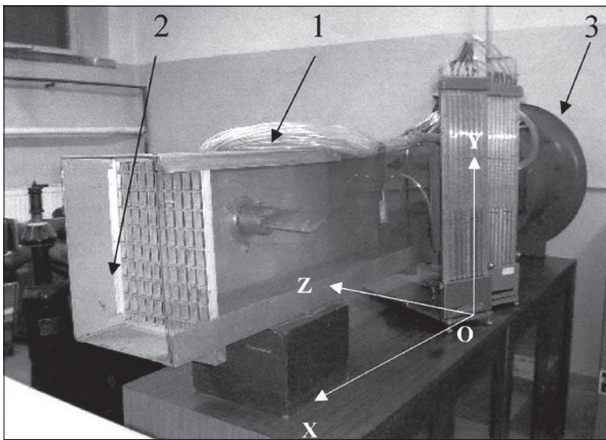


Fig. 1. A view of the negative pressure wind tunnel: 1 – inlet, 2 – hoses connecting measurement point with micromanometers, 3 – fan

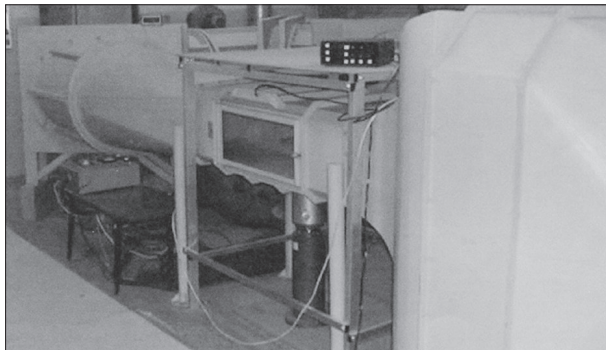


Fig. 2. An overall view of the positive gauge pressure wind tunnel

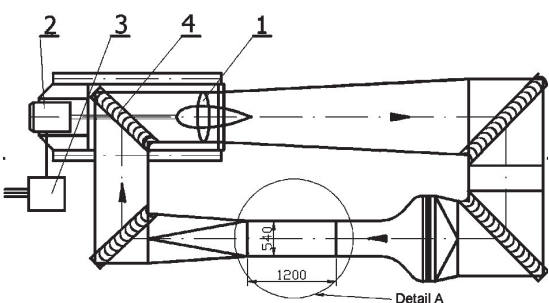


Fig. 3. A diagram of the positive gauge pressure wind tunnel [9]
For details see text

The "A" detail sizes the test passage. In Figures 4 and 5, the diagram and view of a bracket 1 – a vital section of the wind tunnel – are shown. The bracket is used to fix and set tested objects in a wind tunnel 6. Fixing consisted in fastening 5 tested elements into a fixing roller. Setting meant turning a shaft 4, using a knob 3, and the tested object, fixed on the roller, at the same time. *OXYZ* axes determine the setting

space. The object relative to the *OX* and *OY* axes was orientated with the use of the γ angle, whose value was shown on the screen 2 after turning the knob 3. There is positive gauge pressure in the test section of the tunnel.

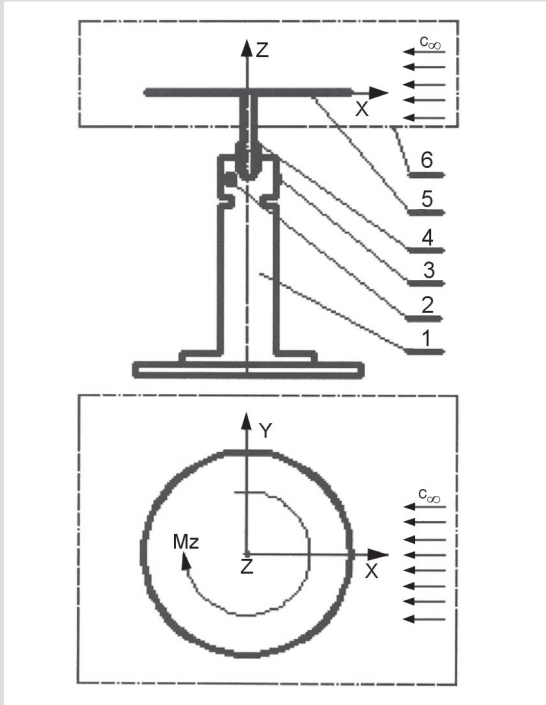


Fig. 4. The test bracket – a diagram

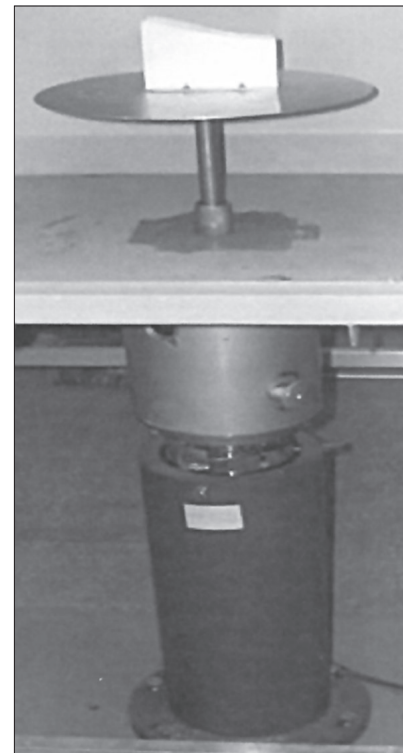


Fig. 5. The test bracket – a view [9]

To construct the blade passage model, two WWOax 22.5 fan blades were used. The blades were designated "a" and "b". Blade dimensions are shown in Figure 6.

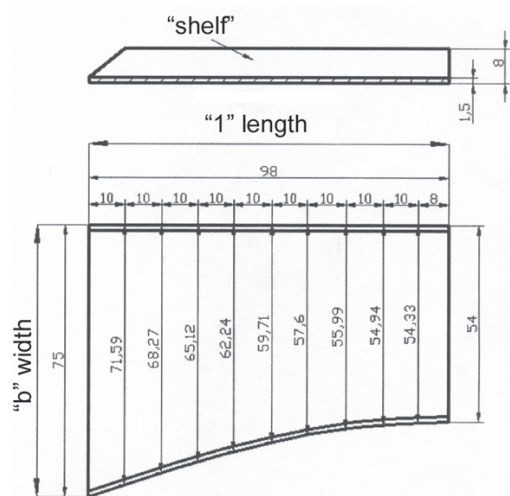


Fig. 6. Dimensions of the flat fan blade

Each blade had so-called "shelves", used to fix it in the fan rim. Sections of the carrying disk and the capping disk were fixed on the "shelves" yielding a closed model of passage.

Figure 7 shows an overall view of the "a" and "b" blades.

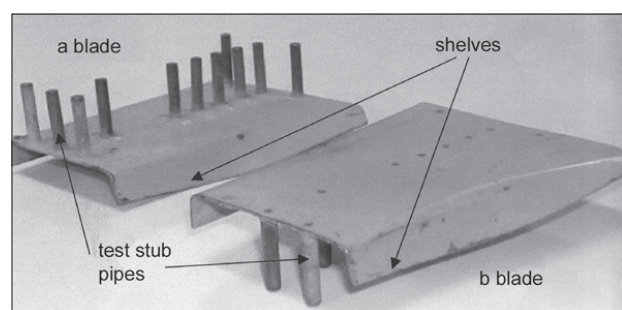


Fig. 7. Fan blades, "a" and "b"

To have test points, 11 holes were made in the blades. The holes were identically distributed in the blades. Their spacing is shown in Figure 8 and test holes coordinates – x_i and z_i – are stated in Table 1.

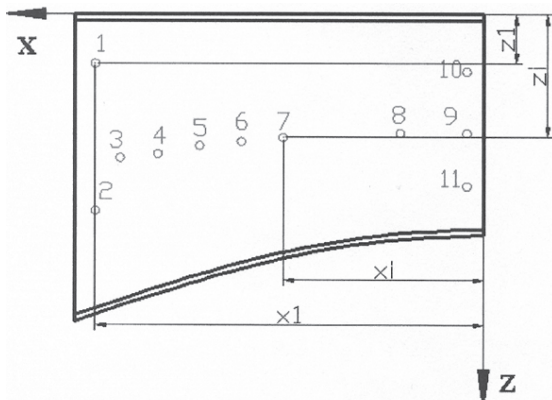


Fig. 8. Spacing of the test holes. 1–11—holes

Table 1

The statement of the test hole coordinates

Coordinates	Test hole determination										
	1	2	3	4	5	6	7	8	9	10	11
x_i , mm	93	93	87	78	68	58	48	20	4	4	4
z_i , mm	12	48	35	34	32	31	30	29	29	14	42

In order to connect rubber hoses to manometers, stub pipes were welded on to the holes. The blade passage model was constructed by setting the blades in the way shown in Figure 9.

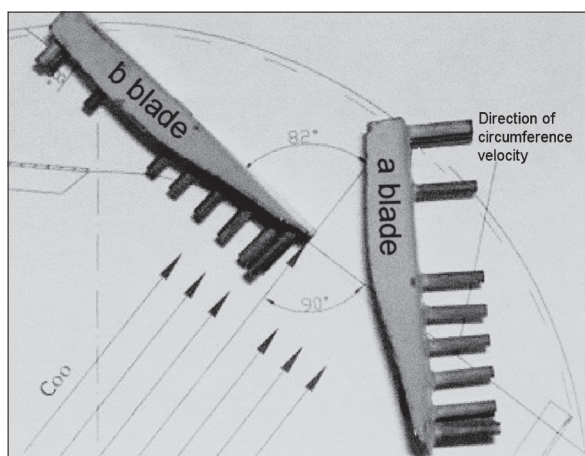


Fig. 9. The blades placed in a blade passage and the principle of determining the zero inlet angle

The flow in the true rotor is axi-symmetric, so the "a" blade is used to measure pressure on the pressure face and the "b" blade to measure it on the suction face of a single blade in the fan rim. The way the blade passage is set relative to the airflow direction in the negative pressure tunnel and positive gauge pressure tunnel is shown in Figure 10. It is in agreement with the assumed orientation of the $OXYZ$ coordinate axes for both test tunnels.

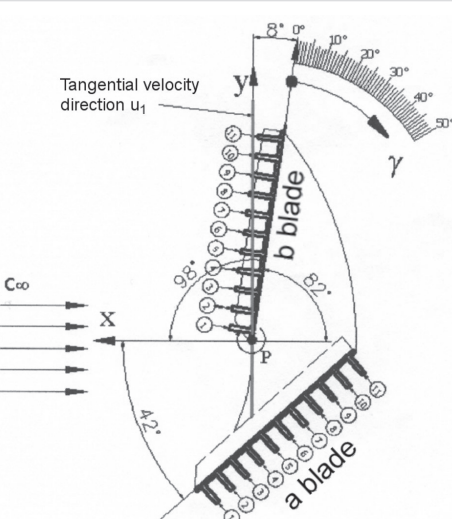


Fig. 10. The principle of blade passage setting and of angle γ orientation

The blade passage in the test tunnel was zero-positioned in the way that enabled the "b" blade to form 82° angle with the airflow direction. In other words, the airflow direction was perpendicular to the rotor tangential velocity u_1 on the "b" blade. Following blade passage positions were diminished to the 45° angle, for which the airflow velocity was parallel to the "a" blade.

3. RESULTS

Knowing pressure distribution on a blade, aerodynamic lift can be calculated using the equation below

$$R_Y = b \int_0^l (p_b - p_a) dl, \text{ N} \quad (1)$$

where:

b – mean blade width, m,

l – blade chord length, m,

p_a – mean nanometric pressure measured on the "a" blade, Pa,

p_b – mean nanometric pressure measured on the "b" blade, Pa.

The lift coefficient, C_Y , for different angles of the blade passage setting in wind tunnels can be calculated due to the aerodynamic lift, R_Y , using the following equation

$$C_Y = \frac{2}{bl c_\infty^2 \rho} R_Y, \quad (2)$$

where:

ρ – air density measured in a wind tunnel, kg/m³,

c_∞ – velocity of undisturbed airflow in a wind tunnel corresponding to the radial component of the velocity in a true rotor, m/s,

R_Y – aerodynamic lift, N.

The results of aerodynamic lift and lift coefficient measurements for various angles of airflow are stated in Table 2.

Figure 11 shows the characteristic of $C_Y = f(\gamma)$ in a negative pressure tunnel and a positive gauge pressure one.

Table 2

The statement of computed aerodynamic lifts and lift coefficients for different angles of γ setting

The blade passage placed in a negative pressure wind tunnel								
c_∞ , m/s	γ	0°	10°	20°	30°	40°	50°	60°
18,1	R_Y , N	1.22	1.32	1.42	1.41	1.2	1.1	0.96
	C_Y , –	1.04	1.11	1.20	1.19	1.02	0.93	0.81
The blade passage placed in a positive gauge pressure wind tunnel								
c_∞ , m/s	γ	0°	10°	20°	30°	40°	50°	60°
14,0	R_Y , N	0.79	0.8	0.81	0.83	0.74	0.71	0.67
	C_Y , –	1.11	1.13	1.14	1.16	1.04	0.99	0.94

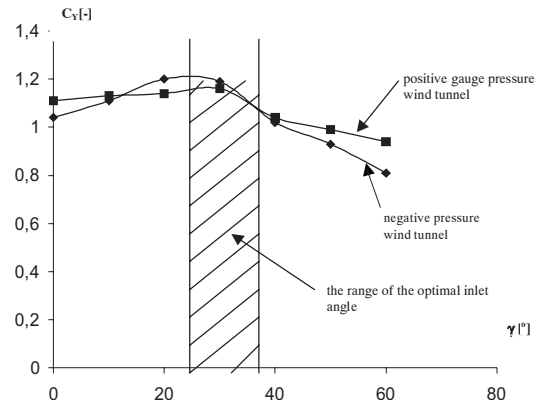


Fig. 11. The characteristic of the $C_Y = f(\gamma)$ blade passage model

4. CONCLUSIONS

The results of this study – stated in Table 2 and Figure 11 – show that the aerodynamic lift acting on the blade passage placed in the negative pressure tunnel and positive gauge pressure tunnel is dependent on the velocity of air feeding the passage. Lift coefficients are constant in both tests if it is assumed that the test error of $\pm 2.3\%$ is admissible. Maximal and minimal measuring deviations are rejected. Other deviations are as follows

$$\delta C_{Yave} = +0.07; +0.02; -0.06; -0.03; +0.02; +0.06; +0.013.$$

The mean deviation is

$$\delta C_{Yave} = \frac{\sqrt{\sum_{i=1}^5 \delta C_Y^2}}{n} = \frac{\sqrt{0.0134}}{5} = \frac{0.115}{5} = \pm 2.3 \text{ %}.$$

In the light of the measuring deviation (error) analysis, the lift coefficient can be said to be the same for tests in the negative pressure wind tunnel and the positive gauge pressure one, and to depend on the angle of air inflow on blade edges. The optimal value of the lift coefficient was determined for angles: $\gamma = 20 \div 30^\circ$. The aerodynamic lift and lift coefficient determined for the model are going to be verified with the results of true fan tests in following studies.

References

- [1] Ciałkowski M.: *Fluid Mechanics*. Poznań, Poznań Technical University Press 2000
- [2] Eck B.: *Ventilatoren*. Berlin, Heidelberg, New York, Springer Verlag 1972
- [3] Eckert B.: *Axial-flow and Radial Compressors*. Warsaw, WNT 1959
- [4] Fortuna S.: *Fan and Compressor Tests*. Cracow, AGH Press 1999
- [5] Grybos R.: *Fluid Mechanics*. Gliwice, The Silesian Technical University Press
- [6] Fortuna S. (ed.): *The Determination of Aerodynamic Lift Acting on the Profile Using the Method of Pressure Distribution*. Instruction (unpublished)
- [7] Troskolański A.T., Łazarkiewicz S.: *Impeller Pumps*. Warsaw, WNT 1973
- [8] Karpel T.: *Research into Losses in Fan Elements*. Cracow (unpublished), 2001
- [9] Gumula S., Knap T.: *The Wind Tunnel of the AGH Department of Power Machines and Facilities*. Cracow, AGH Press 1995